

Fundamentals of tomographic particle image velocimetry

F. Scarano

*Aerospace Engineering Department – Aerodynamics
 Delft University of Technology, 1 Kluiverweg, 2629 HS, Delft, NL*

ABSTRACT

The tomographic PIV technique enables the measurement of fluid motion in a three-dimensional domain. The technique is based on volume illumination and simultaneous imaging of the light scattered by seeding particles from several viewing directions. This work first discusses the new measurement capabilities offered by such configuration in relation to the requirements from fundamental research and applied aerodynamic research. The working principles of Tomo-PIV are then introduced with attention to the illumination and imaging configuration, 3D calibration, object reconstruction and particle motion analysis. The measurement uncertainty analysis can be performed by both theoretical and numerical (synthetic recordings) approaches as well as by *a-posteriori* error estimation for the reconstruction or invoking mass conservation for the velocity vector field.

1 INTRODUCTION

The measurement of the three-dimensional velocity and vorticity fields and their dynamical evolution are of main interest in aerodynamic research in that it enables to visualize for instance 3D vortices, transitional patterns and the spatial organization of coherent structures in turbulent flows. This makes possible a deeper understanding of the complex fluid dynamical mechanism such as vortices interaction and instability mechanisms or the energy transfer between different flow scales in turbulence. Since the identification of vortices and coherent structures relies on the topological operators based on vorticity, or other criteria such as Q - or λ_2 (Hunt *et al.*, 1988; Jeong *et al.*, 1995) it becomes of primary importance to visualize such structures by the measurement of the 3D field of instantaneous velocity and the gradient tensor. Moreover for the evaluation of vortex dynamics the vorticity stretching term $\vec{\omega} \cdot \nabla \vec{V}$ is responsible for the changes in vorticity produced by local intensification (stretching) and reorientation (tilting) of the vorticity of fluid parcels. The quantities of interest for the determination of the flow kinematic properties are summarized below:

$$\vec{V} = \begin{bmatrix} u \\ v \\ w \end{bmatrix}; \quad \vec{\omega} = \begin{bmatrix} \omega_x \\ \omega_y \\ \omega_z \end{bmatrix}; \quad \nabla \vec{V} = \begin{bmatrix} u_x & u_y & u_z \\ v_x & v_y & v_z \\ w_x & w_x & w_z \end{bmatrix}; \quad \vec{\omega} \cdot \nabla \vec{V} = \begin{bmatrix} u_x \omega_x + u_y \omega_y + u_z \omega_z \\ v_x \omega_x + v_y \omega_y + v_z \omega_z \\ w_x \omega_x + w_y \omega_y + w_z \omega_z \end{bmatrix}$$

The planar PIV technique is now well developed for three-component measurement methods by stereoscopy (Arroyo and Greated, 1991). By using two parallel planes, (dual-plane stereo-PIV, Kahler and Kompenhans, 2000) the technique allows the measurement of the velocity derivatives along the direction normal to the plane. Using simultaneously more than two planes has also been demonstrated possible (*X-PIV*, Liberzon *et al.*, 2004).

However the step to the measurement within a complete volume is made difficult by the problem to cope with three-dimensional space from image-based systems, which can only return two-dimensional projections of the physical space. This justifies or at least partly explains the success of the planar PIV technique.

Image-based three-dimensional measurement techniques, require therefore the solution of such problem by “coding” the depth. Fast scanning of the light sheet is suited to flows at low velocity (Brucker, 1995 and Hori and Sakakibara 2004). Holographic PIV allows the instantaneous measurement of relatively large volumes (Herrmann and Hinsch 2004). The 3D-PTV approach visualizes and tracks individual particles trajectories (Virant and Dracos 1997; Schimpf *et al.*, 2003).

2 OPERATING PRINCIPLES OF TOMO PIV

The Tomographic PIV technique as proposed by Elsinga *et al.* (2006) performs the measurement of the particle motion field within a three-dimensional measurement volume by means of the simultaneous view of the illuminated particles by digital cameras placed along several observation directions similarly to the stereoscopic PIV configuration.

Three innovative elements of the technique with respect to the above mentioned 3D methods are introduced:

- a tomographic algorithm is used to reconstruct the 3D particle field from the individual images;
- a 3D calibration procedure directly based on the particle images recordings (Wieneke, 2007);
- three-dimensional cross-correlation with the volume deformation iterative multi-grid technique (VODIM).

2.1 Illumination and imaging

The tracer particles immersed in the flow are illuminated twice by a pulsed light source within a three-dimensional region of space. This is typically achieved by means of light sheet optics producing a thicker sheet (typically up to 20 mm) than for planar PIV. The particle images are recorded from several viewing directions using CCD or CMOS cameras as shown in Figure 1. The Scheimpflug condition between the image plane, lens plane and the median-object-plane has to be fulfilled in order to obtain focused particle images. This is practically achieved by means of camera-lens tilt mechanisms with free orientation of the tilt rotation axis and selecting an appropriate focal depth by the lens aperture. The minimum numerical aperture $f\#$ of the imaging system is dictated by the condition that for the given magnification M_0 and light wavelength λ , the focal depth exceeds the thickness of the illuminated region δz .

$$f\# \geq \left(1 + \frac{1}{M_0}\right) \cdot \sqrt{\frac{\delta z}{4\lambda}} \quad (1)$$

The depth-of-focus criterion limits the optical resolution of the system in that particle tracers are imaged through a relatively small aperture and consequently the image diameter is limited by optical diffraction. For instance, when a measurement volume depth $\delta z = 20$ mm is required and assuming a magnification $M_0 = 0.2$ and a wavelength $\lambda = 0.5 \mu\text{m}$ (green), the resulting value of the numerical aperture is $f\# \approx 16$. As a consequence the diffraction spot d_0 of the system given by the following equation:

$$d_0 = 2.44 f\# (M_0 + 1) \lambda \quad (2)$$

is approximately $25 \mu\text{m}$, which for typical CCD sensors corresponds to 3÷4 pixels. The depth-of-focus criterion, therefore, limits several parameters of the imaging process:

- the light collected by the sensor is reduced in proportion to the square of the numerical aperture
- the relatively large diffraction spot causes the particle images to spread over several pixels, in turn lowering the maximum number of seeding particles that can be imaged at a given image source density.
- the image contrast is strongly diminished being inversely proportional to the 4th power of the numerical aperture as from the combined effect of points *a* and *b*.

Finally, if one considers also the drop in scattered laser light when increasing the sheet thickness (measurement volume depth D), the particle images peak intensity I_{max} finally scales as D^{-5} . Consequently, illumination and imaging over relatively thick volumes (i.e. larger than 10 mm in air and 20 mm in water) have shown to be somewhat problematic in terms of light intensity received by the digital imagers.

2.2 Tomographic reconstruction

The reconstruction of the 3D object from the digital images requires prior knowledge of the mapping function between the image planes and the physical space. This is achieved by means of a calibration procedure similar to that of stereoscopic PIV. However the procedure requires such mapping function to be defined onto a volumetric domain and the requirement for a precise alignment between calibration and measurement plane is not a restriction in this case since no such plane exists for the tomographic technique, which makes it easier to implement the experiment with respect to planar PIV in terms of laser light alignment. However as discussed by Elsinga *et al.*, (2006) the requirement for an accurate relative position between cameras for the tomographic technique is that the mapping function must be accurate within a fraction of the particle image diameter, which is significantly more stringent than that for planar stereo PIV. This is practically achieved by *a-posteriori* correction of the calibration mapping function somehow similarly to the light sheet misalignment technique used in stereo PIV (*self-calibration technique*, Wieneke 2005).

The novel aspect introduced with the Tomographic-PIV technique is the reconstruction of the 3D particle distribution by optical tomography, which deserves a detailed discussion.

The 3D intensity distribution $E(X,Y,Z)$ is discretized as a 3D array voxels elements. The projection of the volume intensity $E(X,Y,Z)$ onto the image at the i^{th} pixel position (x_i, y_i) returns the pixel intensity $I(x_i, y_i)$. By linear approximation the projection is obtained as superposition (sum) of the intensity along the line of sight, which is mathematically expressed by a set of linear equations:

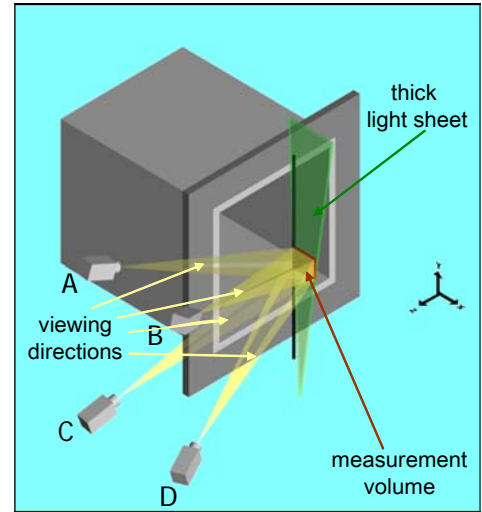


Figure 1 - Schematic principle of tomographic PIV data processing

$$\sum_{j \in N_i} w_{i,j} E(X_j, Y_j, Z_j) = I(x_i, y_i) \quad (3)$$

where N_i is the ensemble of voxels (typically from a $3 \times 3 \times 3$ kernel) neighbouring the j^{th} voxel around the line of sight associated to the i^{th} pixel (x_i, y_i) through the volume. The coefficient $w_{i,j}$ weights the contribution of the j^{th} voxel with intensity $E(X_j, Y_j, Z_j)$ to the pixel intensity $I(x_i, y_i)$ and is calculated as the fraction of volume intersecting the voxel and the line of sight. Such system is highly underdetermined for tomo-PIV, where only a few viewing directions (equations) are available and the number of unknowns (intersected voxels) is large (in the order of the sensor size).

A solution of the problem defined by eq. 3 may be obtained by an inverse approach. The multiplicative algebraic reconstruction technique (MART), from Herman and Lent, 1976) allows solving iteratively the given system of equations. Starting from an initial guess $E_0(X, Y, Z)$, uniform and non-zero, the object $E(X, Y, Z)$ is updated at each iteration in a loop over each pixel i from all cameras and each voxel j as:

$$E_{k+1}(X_n, Y_n, Z_n) = E_k(X_n, Y_n, Z_n) \cdot \left(\frac{I(x_m, y_m)}{\sum_{n=1}^N W_{m,n} E_k(X_n, Y_n, Z_n)} \right)^{\mu W_{m,n}} \quad (4)$$

where $\mu \leq 1$ is a scalar relaxation parameter and its unit value ensures the fastest convergence rate. The magnitude of the update is determined by the ratio of the measured pixel intensity I with the projection of the current object $\sum_{j \in N_i} w_{i,j} E(X_j, Y_j, Z_j)$. The exponent again ensures that only the elements in $E(X, Y, Z)$ affecting the i^{th} pixel are updated. Furthermore the multiplicative MART scheme requires that E and I are definite positive.

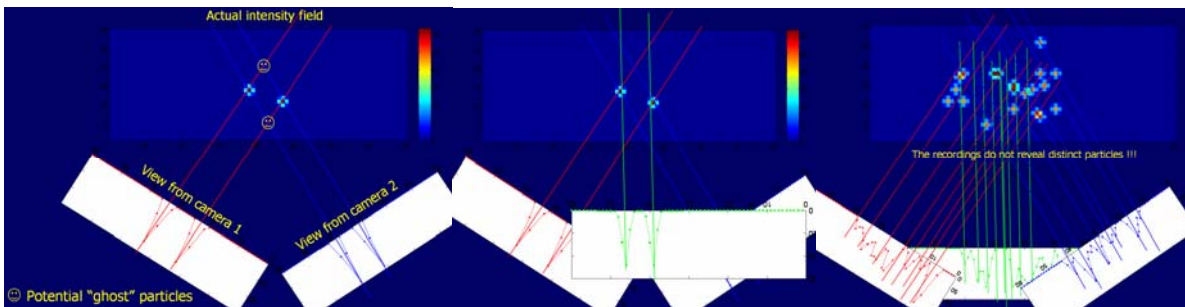
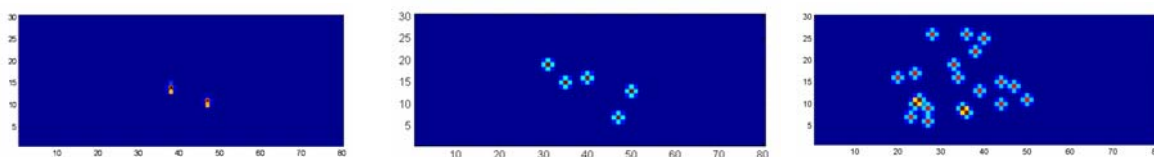


Figure 2 – Imaging of 3D particle field. Left: two views for two particles yield four potential reconstruction. Centre: adding a third view eliminates simultaneous spurious intersections (ghost particles). Right: seeding density not allowing particles to be imaged distinctly.

Figure 2 and Figure 3 provide a visual description of the imaging process and the iterative reconstruction for different configurations. When a set of two particles is imaged by two cameras, four possible particles are the solution of the reconstruction algorithm. This problem is referred to as *ghost particles*. Introducing a third viewing direction completely solves the ambiguity. When the particles are projected onto well distinct images on the sensors, an accurate reconstruction is possible as shown in Figure 2-centre. The iterative MART approach enables to obtain reconstruction accuracy significantly higher than that obtained by a simple multiplication of the projected light intensity as shown in Figure 3. However, when individual particle images cannot be properly identified, even the iterative reconstruction is not accurate.



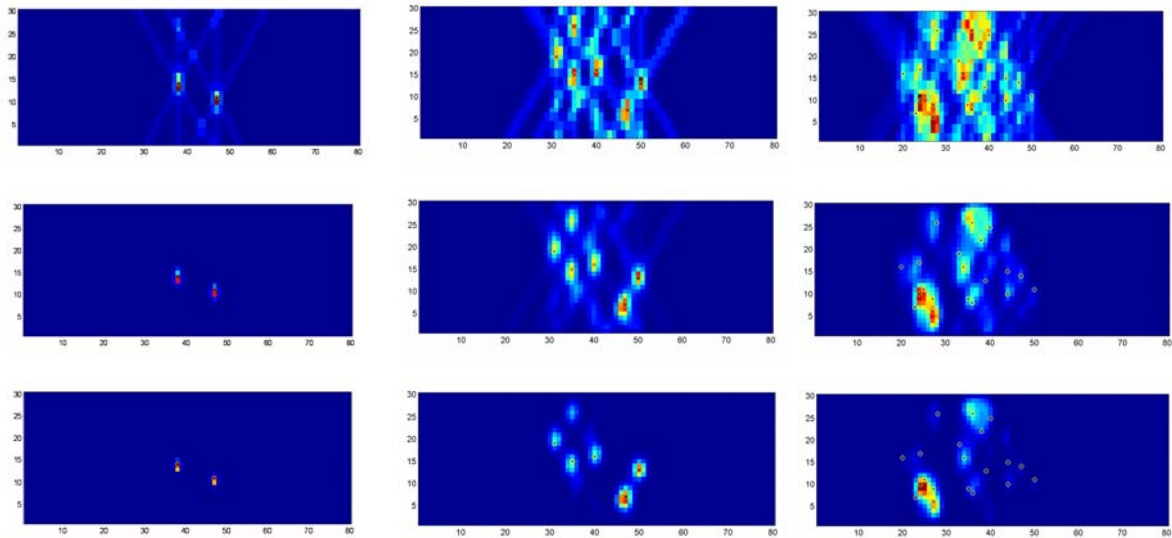


Figure 3 – Actual particle distribution (top row) and reconstructed intensity field with 3 coplanar views. After 1 (2nd row), 3 (3rd row) and 5 (4th row) MART iterations

A quantitative analysis from computer-generated particle images corresponding to a known 3D particle field from which a tomographic reconstruction allows to estimate the correlation coefficient Q between the reconstructed and the actual intensity. Therefore the accuracy of the reconstruction can be estimated. Figure 4 shows the evolution of the reconstruction accuracy as a function of the MART iterations. The increase rate of Q after five iterations has decreased of approximately two orders of magnitude with respect to the first update. This is particularly interesting since the reconstruction procedure is computationally intensive and is a substantial portion of the computational effort due to data processing. Furthermore experimental results show that with additional iterations the measured velocity vector field changes only within the noise level. The dependence of the reconstruction accuracy upon the seeding density (expressed in particles/pixel) is crucial as shown in Figure 4. A system with only two views is rather inadequate to perform tomographic measurements, whereas a typical value of the seeding density is 0.02 for a three-views system. The most common option adopted in several experiments is to use a set of four simultaneous views, which allows approximately a seeding density of 0.05 (50,000 particles/Mpixel). Additional details of these numerical simulations are reported in Elsinga *et al.* (2006). Increasing further the number of cameras makes the reconstruction accuracy less sensitive to the seeding density, however other factors such as system complexity and cost, may pose severe limits to this option.

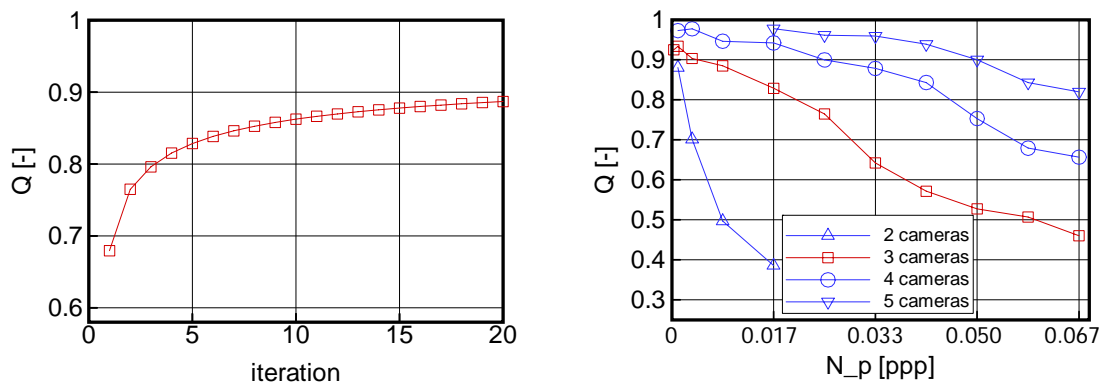


Figure 4 – Reconstruction accuracy as a function of the number of MART iterations (left) and of the seeding density and number of simultaneous views (right) (after Elsinga *et al.* 2006).

2.3 3D MOTION EVALUATION

The method used to extract the displacement from two successively acquired pictures is now well established from planar PIV experiments and it can be summarised with a sequence of steps. First the picture is divided into several small windows (windowing), which may also overlap with each other. Then for each pair of corresponding windows, the following operations are applied:

1. the 2D or 3D fast Fourier transform (*FFT*) of both windows is calculated
2. the *cross product* of the first window *FFT* and the second window *FFT* conjugate is computed
3. the *IFFT* of the result is determined
4. the *location of the maximum is found* and an estimated at a sub-pixel level in the correlation plane is produced by a Gaussian fit
5. the *velocity* is computed by knowledge of the magnification factor and the time separation between exposures

The application of the *FFT* algorithm is not essential to compute the cross-correlation, but it represents a faster alternative to the direct application of the algebraic cross-correlation operator. The parameters that mostly influence the measurement uncertainty are the number of particle pairs in the interrogation windows, the velocity gradient and the particles image size with respect to the spatial discretization. Also the peak interpolation scheme is known to be important in relation to the bias error.

For 3D data structure obtained from tomographic reconstruction of simultaneous views the evaluation of the particle pattern displacement must performed by means of 3D spatial cross correlation analysis. The normalized cross-correlation function $R(\Delta X, \Delta Y, \Delta Z)$ between the intensity field E reconstructed from the recordings at time instants separated by the interval Δt may be regarded as a straightforward extension of the 2D procedure:

$$R(l, m, n) = \frac{\sum_{i,j,k=1}^{I,J,K} E(i, j, k, t) \cdot E(i-l, j-m, k-n, t + \Delta t)}{\sqrt{\text{cov}(E(t)) \cdot \text{cov}(E(t + \Delta t))}} \quad (5)$$

Where the triplet (l, m, n) discretizes the space of 3D shifts $(\Delta X, \Delta Y, \Delta Z)$. The analysis performed with an iterative pattern deformation technique (*WIDIM*, Scarano and Riethmuller, 2000) allows to compensate for any out-of-pattern motion due to the particles velocity and its gradient by means of a mutual transformation of the 3D particle patterns according to a continuous piece-wise linear displacement predictor. In this specific case, the well-known problem of the out-of-plane motion in planar experiments is basically eliminated and the deformation technique enables to recover most of the particle pairs between the two exposures. The Volume Deformation Iterative Multigrid technique (*VODIM*), is the 3D extension of the above method by which the interrogation boxes are displaced/deformed on the basis of the result from the previous interrogation. The intensity field of the deformed volume at the $k+1^{\text{th}}$ iteration is therefore obtained from the original intensity and the predictor velocity field according to the expression:

$$\begin{aligned} E^{k+1}(X, Y, Z, t) &= E\left(X - u_d^k/2, Y - v_d^k/2, Z - w_d^k/2, t\right) \\ E^{k+1}(X, Y, Z, t + \Delta t) &= E\left(X + u_d^k/2, Y + v_d^k/2, Z + w_d^k/2, t + \Delta t\right) \end{aligned} \quad (6)$$

Where $\vec{V}_d^k = (u_d^k, v_d^k, w_d^k)$ represents the particle pattern deformation field obtained at the k^{th} interrogation obtained by tri-linear interpolation of the displacement field at the previous iteration. Between subsequent iterations low pass filtering by 2nd order least-squares regression is applied to the velocity field for process stabilization (Schrijer and Scarano, 2008).

3 UNCERTAINTY ANALYSIS

The main sources of uncertainty for the tomographic technique are associated to the following operations:

- 1) calibration of the imaging system
- 2) tomographic reconstruction
- 3) particle motion estimation

The calibration procedure is performed similarly to that of stereo-PIV. The remaining errors due to incorrect pattern motion and to additional misalignments can be corrected a-posteriori by the self-calibration procedure (Wieneke, 2007). Many tomographic experiments are performed with a typical camera misalignment after the standard calibration, exceeding 1 pixel, which would result in unacceptable errors in the object reconstruction. Using the self-calibration procedure the cameras residual misalignment can be reduced to 0.1 pixels, which is rather acceptable for the purpose of tomographic reconstruction.

The uncertainty associated to the MART tomographic reconstruction has been studied by Elsinga et al. (2006) and depends essentially upon the number of MART iterations, on the number of independent views and the viewing solid angle, on the particle seeding density, particle diameter, background illumination and camera noise. Therefore from the above parameters it is possible to perform an optimization of the tomographic measurement. A simple and practical a-posteriori evaluation of the tomographic reconstruction quality is based on the comparison between the light intensity

level reconstructed in the illuminated region with respect to that outside. A clear transition between illuminated and not illuminated regions as shown in Figure 5 is the necessary condition for an accurate reconstruction.

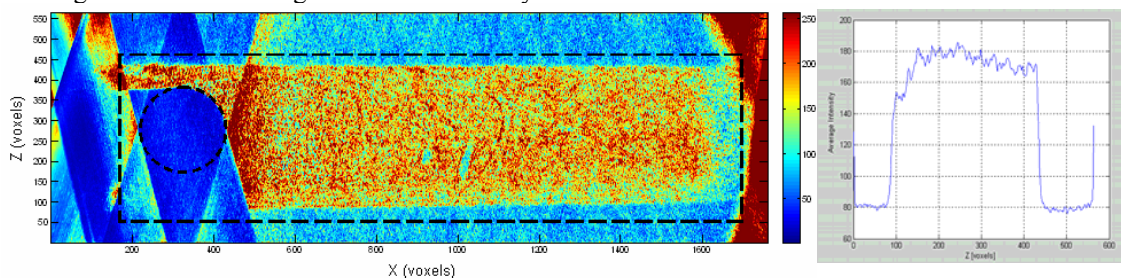


Figure 5 – Cross-sectional projection of the reconstructed object (left) and corresponding intensity distribution along the depth (right)

Finally, the uncertainty associated to the motion estimation can in first approximation, be deduced from rules and criteria obtained for planar PIV. The typical error level for 3D cross-correlation operator ranges from 0.1 to 0.2 voxels and depends upon the size of particle images and the accuracy of the reconstruction itself. The most straightforward *a-posteriori* error estimate may be based on the residual of the continuity equation (solenoidal velocity field) or on the residual of the vorticity equation for time resolved experiments.

4 CONCLUSIONS

The principles of three-dimensional particle image velocimetry by tomography are presented. This technique is based upon the simultaneous view of particles illuminated within a measurement volume. The measurement configuration is similar to that used for stereo-PIV as well as the calibration procedure, except for the correction of calibration errors that need a specific 3D algorithm since the disparity error is not defined within a plane. The main advantage offered by the tomo-PIV technique with respect to alternative methods is that it is suited for high seeding density (50,000 particles/megapixel), easily applies to high-speed flows and the measurement setup is relatively straightforward. The main limitations are the small aspect ratio between depth and width of measurement domain (typically 1:4) and the computational effort needed for the 3D reconstruction and motion evaluation.

Acknowledgements

Work supported by the Dutch Technology Foundation STW-VIDI grant DLR.6198.

References

- Arroyo MP and Greated CA (1991) "Stereoscopic particle image velocimetry", *Meas Sci Technol*, 2, 1181-1186
- Elsinga GE, Wieneke B, Scarano F and van Oudheusden BW (2006) "Tomographic particle image velocimetry", *Exp. Fluids*, 41, 933-947
- Herrmann SF and Hinsch KD (2004) "Light-in-flight holographic particle image velocimetry for wind-tunnel applications", *Meas. Sci. Technol.* 15, 613-621
- Hori T and Sakakibara J (2004) "High-speed scanning stereoscopic PIV for 3D vorticity measurement in liquids", *Meas. Sci. Technol.* 15, 1067-1078
- Kähler CJ and Kompenhans J (2000) "Fundamentals of multiple plane stereo particle image velocimetry", *Exp Fluids*, S70-S77
- Liberzon A, Gurka R and Hetsroni G (2004) "XPIV-multi-plane stereoscopic particle image velocimetry", *Exp Fluids* 36, 355-362
- Pereira F, Gharib M, Dabiri D and Modarress M (2000) "Defocusing PIV: a three-component 3-D PIV measurement technique. Application to bubbly flows", *Exp. Fluids, Suppl.* 29, S78-S84
- Scarano F (2002) "Iterative image deformation methods in PIV", *Meas. Sci. Technol.* 13, R1-R19
- Scarano F, Elsinga GE, Bocci E and van Oudheusden BW (2006) "Investigation of 3-D coherent structures in the turbulent cylinder wake using Tomo-PIV", 13th Int. Symp. Appl. Laser Tech. Fluid Mech., Lisbon, PT
- Schimpf A, Kallweit S, Richon JB (2003) "Photogrammetric particle image velocimetry", 5th Int. Symp. on particle Image Velocimetry, Busan, Korea
- Schrijer FFJ and Scarano F (2006) "On the stabilisation and spatial resolution of iterative PIV interrogation", 13th Int. Symp. Appl. Laser Tech. Fluid Mech., Lisbon, PT
- Virant M and Dracos T (1997) "3D PTV and its application on Lagrangian motion", *Meas. Sci. Technol.*, 8: 1539-1552
- Wieneke B (2005) "Stereo-PIV using self-calibration on particle images", *Exp. Fluids* 39, 267-280
- Wieneke B (2007) "Volume self-calibration for tomographic PIV", Dagstuhl Workshop, Wadern, DE